Electron spin resonance studies and theoretical quantum calculations of free radicals generated from anthracenetrione by electrochemical and microsomal reduction

Claudio Olea-Azar [a,*], Fernando Mendizábal [b], Jaime Alarcón [a], Rodolfo Briones [a], Bruce K. Cassels [b], Tomás Delgado-Castro [c], Ramiro Araya-Maturana [c]

[a] *Departamento de Química Inorgánica y Analítica, Facultad de Ciencias Químicas y Farmacéuticas, Universidad de Chile, Casilla 233, Santiago 1, Chile*

[b] *Departamento de Química, Facultad de Ciencias, Universidad de Chile, Casilla 233, Santiago 1, Chile*

[c] *Departamento de Química Orgánica y Fisicoquímica, Facultad de Ciencias Químicas y Farmacéuticas, Universidad de Chile, Casilla 233, Santiago 1, Chile*

Abstract

The ESR spectra of radicals obtained by electrolytic reduction of 4,4-dimethylanthracene-1,9,10 (4H)-trione (**1**) and the regioisomeric quinones 8-acetyloxymethyl-4,4,5-trimethyl- (**2**), and 5-acetyloxy-methyl-4,4,8-trimethyl-(4H)-1,9,10-anthracenetrione (**3**) were measured in DMSO and analyzed by quantum chemical calculations. The electrochemistry of these compounds was characterized using cyclic voltammetry, in DMSO and DMF solvents and compared with nifurtimox. The quinones were also reduced by microsomal NADPH-cytochrome P-450 reductase and the corresponding radicals species were also detected by ESR spectroscopy. AM1, INDO, and ADF calculations were performed to obtain the optimized geometries, theoretical hyperfine constants, and spin distributions, respectively. Density functional theory was used to rationalize the reduction potential of these compounds.

Keywords: ADF; Cyclic voltammetry; ESR; INDO; Quinone anion radical; *T. Cruzi*

1. Introduction

The electrochemical behavior of funtionalized quinones is an important characteristic closely linked to biological properties, such as the inhibition of redox enzymes. In fact, some natural and synthetic quinones showing activity against the

* Corresponding author. Tel.: + 56-2-6782846; fax: + 56-2-7370567.

E-mail address: colea@uchile.cl (C. Olea-Azar).

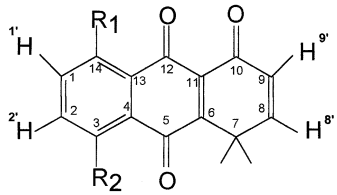

Quinone	R_1	R_2
1	H	H
2	CH_3	CH_2OAc
3	CH_2OAc	CH_3

Fig. 1. Chemical structure of the anthracenetriones.

protozoon *Trypanosoma cruzi*, the causative agent of Chagas' disease, may exert their action primarily by upsetting the parasite's antioxidative defense mechanisms through interaction with the enzyme trypanothione reductase [1], or by disrupting mitochondrial electron transport [2,3].

The activities of many presently used antichagas drugs involve intermediate one electron reduction products (i.e. free radicals), which are the active species [4]. Recently, we have reported ESR studies on antichagasic activities of nitrocompounds which are analogues of nifurtimox [5] and N-oxide derivatives [6], which showed in their reduction mechanisms, stable radical species which are more active than nifurtimox [7].

Also, it has been shown that the V/K_m ratio for a series of simple quinones undergoing reduction by trypanothione reductase decreases by about three orders of magnitude as the one-electron reduction potentials fall from 0.09 V to -0.26 V [8], and that the trypanocidal activity of heterocyclic and 2-hydroxynaphtoquinones is only a constant characteristic when the first cathodic potential Ep_{c1} is more positive than -0.72 V [9]. Nevertheless, structural variants of compounds with similar electrochemical potentials may be expected to exhibit very different biological activities, especially in their interactions with enzymes, which as a rule impose severe structural demands on inhibitors or substrates [10].

The unsubstituted 4,4-dimethyl-(4H)-anthracene-1,9,10-trione [11], exhibits potent lytic activity in vitro against *T. cruzi* and several *Leishmania* species [12]. As computational docking studies using a model of trypanothione reductase had suggested that the introduction of oxymethyl substituents at C-5 or C-8 of this structure might exhibit greater affinity for the enzyme's active site [13], precursors of such derivatives were prepared by Diels–Alder reactions of 8,8-dimethylnaphthalene-1,4,5(8H)-trione with appropriate dienes [14].

In the present work, we report electrochemical studies of 4,4-dimethylantracene-1,9,10 (4H)-trione (**1**) and the regioisomeric quinones 8-acetyloxymethyl-4,4,5-trimethyl- (**2**), and 5-acetyloxy-methyl-4,4,8-trimethyl-(4H)-1,9,10-

Table 1
Cyclic voltammetric parameters of antracenetrione derivatives versus saturated calomel electrode

Quinone	E_{pc1}/V	E_{pa1}/V	ΔE/V	$E_{1/2}$/V	E_{pc2}/V	E_{pa2}/V	ΔE/V	$E_{1/2}$/V
1								
DMSO	−0.46	−0.39	0.07	−0.45	−0.90	−0.81	0.09	−0.86
DMF	−0.45	−0.38	0.06	−0.42	−0.82	−0.66	0.16	−0.74
2								
DMSO	−0.58	−0.52	0.06	−0.55	−1.12	−1.00	0.12	−1.06
DMF	−0.61	−0.55	0.06	−0.58	−1.12	−0.90	0.22	−1.01
3								
DMSO	−0.59	−0.53	0.06	−0.56	−1.13	−1.00	0.13	−1.07
DMF	−0.59	−0.53	0.06	−0.56	−1.03	−0.91	0.12	−0.97
NIFURTIMOX								
DMSO	−0.91	−0.85	0.06	−0.88	−1.60	–	–	
DMF	−0.89	−0.84	0.05	−0.87	−1.30	–	–	

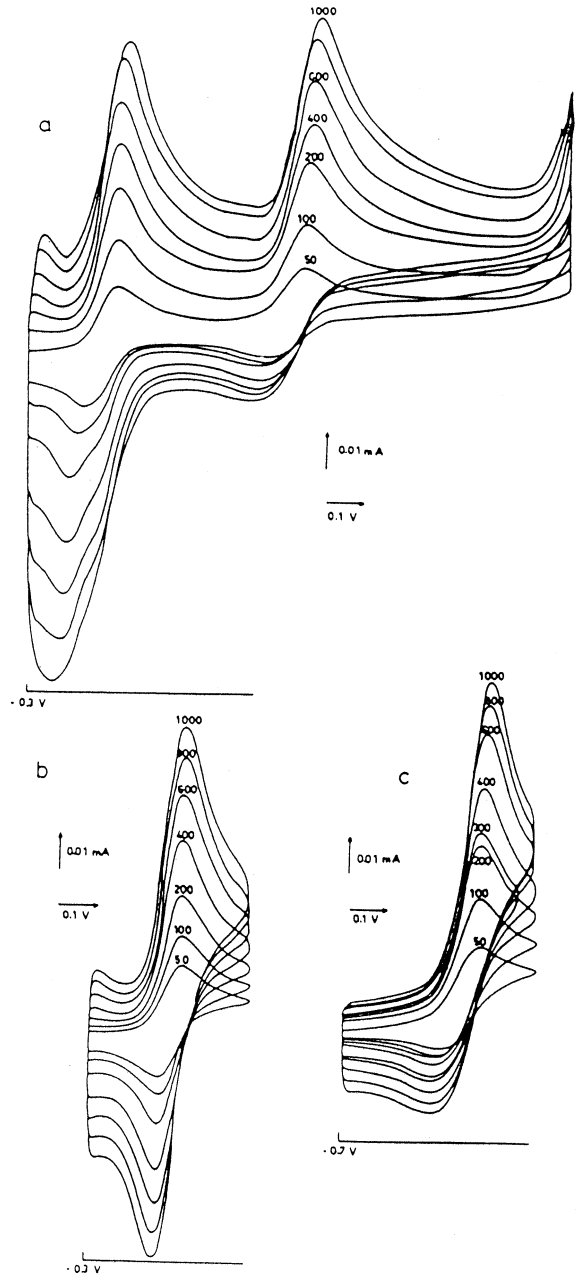

Fig. 2. (a) Cyclic voltammetry of quinone 2 in DMSO at different sweep rates. (b) Isolated first couple at different sweep rates. (c) Isolated second couple at different sweep rates.

anthracenetrione (**3**) (Fig. 1) in dimethylsulfoxide (DMSO) and dimethylformamide (DMF). The formal one electron transfer potential for the new quinines was compared with that of nifurtimox. The anion radicals produced in the electrochemical process were characterized by ESR. The quinone derivative radicals were also generated by a microsomal system.

To estimate the theoretical hyperfine constants, INDO-SCF calculations were carried out. The geometry of each compound in both spin-paired and free radical forms was fully optimized by AM1 methodology

Finally, we have applied the approximate density functional theory (DFT) using the Amsterdam density functional (ADF) program to obtain the electron affinities of these compounds.

2. Experimental

2.1. Samples

The anthracenetrione were synthesized according to methods described earlier [13].

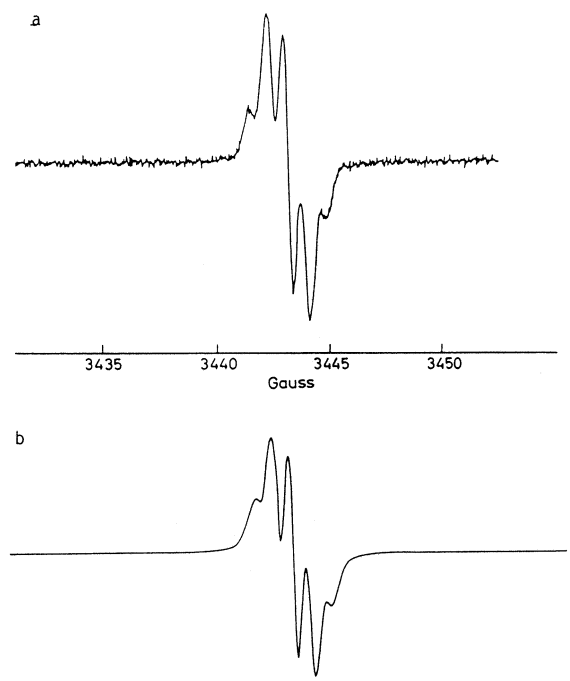

Fig. 3. (a) ESR experimental spectrum of anion radical of quinone 2 in DMSO. (b) Computer simulation of the same spectrum.

Table 2
Experimental and theoretical hyperfine splittings (Gauss) and g values for the quinones anion radicals studied in DMSO

QUINONE	aH_1, aH_2	aH_8, aH_9	aH (R1, R2 = H)	aH (CH3)	g values
1					
EXP	0.65 0.65	0.60 0.60	1.30 1.30	0.18	2.0053
INDO	0.62 0.67	0.59 0.57	1.20 1.15	0.14	
2					
EXP	0.60 0.60	0.90 0.90	–	0.23	2.0048
INDO	0.63 0.65	0.98 0.92		0.15	
3					
EXP	0.95 0.45	1.06 1.06	–	0.23	2.0050
INDO	0.90 0.60	1.00 0.99		0.18	

2.2. Cyclic voltammetry

The DMSO and DMF (spectroscopy grade) were obtained from Aldrich. The tetrabutylammonium perchlorate (TBAP) used as supporting electrolyte was obtained from Fluka. Cyclic voltammetry was carried out using a Weenking POS 88 instrument with a Kipp Zenen BD93 recorder, in DMSO or DMF (ca 1.0×10^{-3} mol dm^{-3}), under a nitrogen atmosphere, with TBAP (ca 0.1 mol dm^{-3}), using three-electrode cells. A mercury-dropping electrode was used as the working electrode, a platinum wire as the auxiliary electrode, and saturated calomel as the reference electrode. The semiquinone radicals were generated by electrolytic reduction in situ at room temperature.

2.3. ESR spectroscopy

ESR spectra were recorded in X band (9.85 GHz) using a Bruker ECS 106 spectrometer with a rectangular cavity and 50 KHz field modulation. The hyperfine splitting constants were estimated to be accurate within 0.05 G.

2.4. Microsomal experiment

The experiment was run in a Tris buffer (150 mM KCl, 50 mM Tris–HCl, pH 7.36 at 25°C) that was treated with Chelex ion exchange resin before use to remove adventitiously present metal ions. The NADPH, NAD, glucose-6-phosphate and glucose-6-phosphate dehydrogenase were obtained from Sigma. All chemicals were dissolved in the buffer (minimal quantities of DMSO, as was necessary for the anthradecetrione derivatives). Incubations consisted of microsomes homogenized in buffer (typically 3 mg of protein/ml), Anthracenetrione derivatives (5.0 mM) glucose-6-phophate (10 mM) with glucose-6-phophate dehydrogenase as an NADPH-generated system, and NADPH (1mM). The rat liver

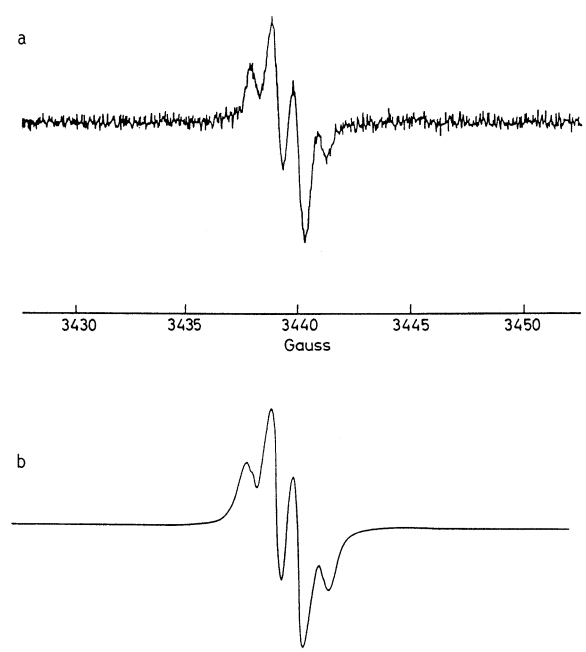

Fig. 4. (a) ESR spectrum of quinone 3 generated by microsomal system. (b) Computer simulation of the same spectrum.

Table 3
Selected dihedral angles for the quinones studied

System	Electronic state	<14-13-12-11	<14-13-4-5	<12-11-10-9	<13-12-11-10
Quinone 1	Neutral	166	179	164	158
	Radical	162	178	166	156
Quinone 2	Neutral	156	179	175	145
	Radical	149	179	179	154
Quinone 3	Neutral	147	177	169	141
	Radical	146	179	174	144

microsome were prepared by published methods and kept frozen at -70°C until used. Buffer was added if necessary to maintain a constant total volume for all experiments. In all cases, the NADPH was added immediately before the EPR spectrum was taken.

2.5. Theoretical calculations

Full geometry optimizations of these quinones in spin-paired and free radical forms were carried out by AM1 methods [15]. INDO calculations were done employing the open shell UHF option. The electron affinities were calculated using ADF calculations. This approach solves the Kohn–Sham equations within the local density approximation (LDA) with gradient corrections for the exchange and correlation potentials. The ADF basis set used was a doublet-ξ plus polarization functions. The LDA exchange correlation suggested by Vosko and Wilk [16] was used. The nonlocal gradient corrections for exchanges proposed by Becke and the nonlocal correction for correlation proposed by Perdew [17] were used.

3. Results and discussion

3.1. Cyclic voltammetry

Table 1 lists the values of the voltammetric peaks and the anodic and cathodic currents for the three compounds. These quinones displayed comparable voltammetric behavior, showing two well-defined reduction waves in DMSO or DMF.

The first wave for both quinones studied corresponded to a reversible one-electron transfer. The

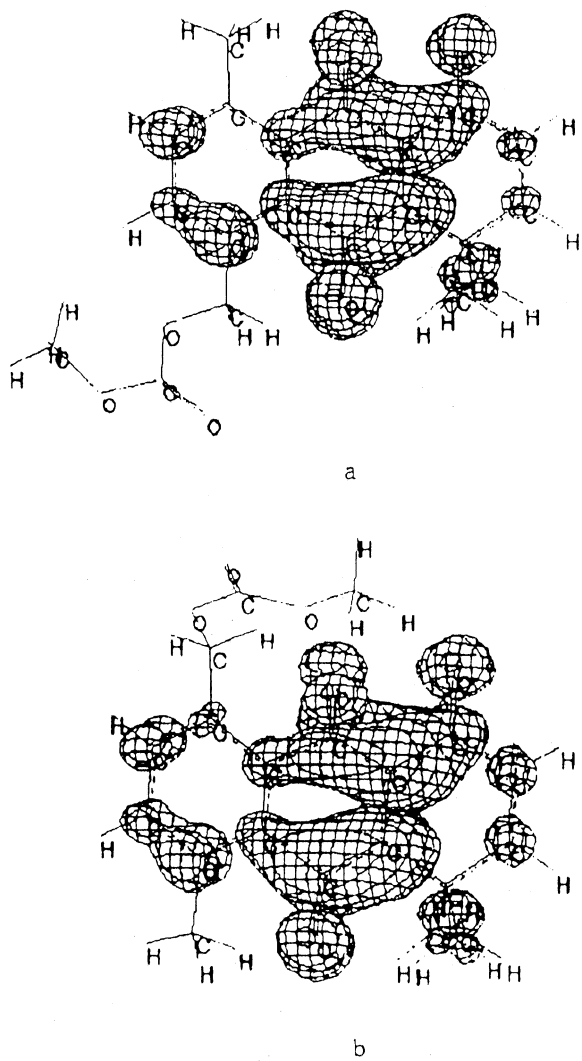

Fig. 5. (a) Electron spin density of SOMO quinone 2. (b) Electron spin density of SOMO quinone 3.

Table 4
Electron affinities (eV) and reduction potential (in DMSO)

Quinone	LDA	LDA + NLC (Becke-Perdew)	$E_{1/2}$
1	−0.998	−0.948	−0.45V
2	−0.713	−0.697	−0.55V
3	−0.700	−0.690	−0.56V

reverse scan showed the anodic counterpart of the reduction waves (Fig. 2b). The breadth of the cathodic wave at its half intensity has a relatively constant value of 60 mV. The intensity ratio ip_a/ip_c has a value close to unity. According to the standard reversibility criteria, this couple corresponds to a reversible diffusion-controlled one-electron transfer. It is attributable to the reduction of quinone to semiquinone, a stable anion radical at room temperature. The second couple is quasireversible over the whole range of sweep rates used (50–1000 V/s) (Fig. 2b). We can attribute this wave to the production of a hydroquinone derivative. It can be seen that these quinones possess an Ep_c in the range described for quinones displaying activity against *T. cruzi* [9]. The electrochemical data were very similar for all compounds, so that cyclic voltammetry is unable to distinguish the regioisomeric compounds.

3.2. Electron spin resonance

The semiquinone free radicals were prepared in situ by electrochemical reductions in DMSO, applying a potential corresponding to the first wave for the quinones as obtained from the cyclic voltammetric experiments. The interpretation of the ESR spectra by means of a simulation process has led to the determination of the coupling constants for all the magnetic nuclei, confirmed by theoretical calculations.

The ESR spectrum of quinone **1** was analyzed and simulated in term of three triplets from the three groups of two equivalent hydrogen nuclei and a septet from six equivalent hydrogens due to two methyl groups (not shown here).

The reduction products of the regioisomeric quinones **2** and **3** showed slight differences on the hyperfine splitting patterns. The ESR spectrum of the semiquinone radical obtained from **2** was analyzed and simulated in terms of two triplets from the two groups of two equivalent hydrogen nuclei, and a septet from six equivalent hydrogens belonging to the two methyl groups (Fig. 3). The spectrum of the radical derived from quinone **3** was also well resolved. This spectrum was simulated in terms of one triplet due to two equivalent hydrogens. The hydrogens arbitrary numerated as 1′ and 2′ showed slight differences in the hyperfine constants, and a septet from six equivalent hydrogens belonging to the two methyl groups. However, few lines appear due to the bigger experimental broad line (not shown here). In order to simulate the ESR spectra, the same hyperfine constants and numbers of proton obtained in the experimental results were utilized. The linewidth used to obtain the same shape was 0.45 G. The hyperfine splitting constants are listed in Table 2. The difference in the hyperfine pattern obtained to quinines 2 and 3 are able to distinguish both regioisomers.

The microsomal incubations of all compounds gave an ESR spectrum, after a brief induction period of 1–2 min that was required for the incubation to become anaerobic. Fig. 4 shows the ESR spectrum of quinone 3 and its corresponding simulation spectrum. The hyperfine splitting of the radicals was the same than that obtained by electrochemical reduction. Also, we produced the stable radicals quinone 1 and 2 generated by microsomal system, which presented the same hyperfine splitting as the electrochemical generation system.

4. Theoretical calculations

We fully optimized the geometries for the electron-paired and anion radical molecules at AM1 level. All radical structures showed small distortion, relative to the neutral analogue molecules. Dihedral angles are summarized in Table 3, in order to rationalize the difference in the hyperfine patterns of the quinone 2 and 3. The more planar structure of quinone 3 was in agreement with a more homogenous spin distribution, which is observed through the equivalent hyperfine constants.

ADF level calculations were done in order to obtain the Mulliken's analysis of the SOMO anion radicals. These structures showed that 50% of the unpaired electron is distributed in the ring structure and the other half is localized in the three carbonyl oxygens. In particular, the oxygen bonded to C5 accumulates approximately 25% of this distribution, while the oxygen bonded to C10 has 15%, and finally the oxygen connected to C12 had the remaining 10%.

The spin density distributions of quinone radicals 2 and 3 are shown in Fig. 5. Both diagrams described a similar distribution, however the strongest difference can be appreciated in the C1 and C2 atoms. Meanwhile, the quinone 2 showed a spin density distribution between C1 and C14, in the quinone 3 this property is only located in C1 atom. These results are in agreement with the small difference observed in the experimental hyperfine constants $aH_{1'}$ and $aH_{2'}$ found in the quinone 3.

INDO/1 calculations were performed in order to obtain the theoretical hyperfine constants, using the geometries from AM1 calculations. Table 2 shows both the experimental and calculated hyperfine constants. The results are in agreement with the assignment of the hyperfine constants.

In order to estimate the ability of the molecules to accept electrons, the electron affinities were calculated using ADF and comparisons were made with the formal reduction potentials of the anion radical forms (Table 4). The calculations show that the electron affinities of these quinones correlate well with the experimental value estimated from the reduction potentials.

5. Concluding remarks

All quinones studied possessed an Epc in the range described for quinones displaying activity against *T. cruzi*. Also, these quinones showed lower Epc than nifurtimox which is the clinical drug used in Chagas disease.

Stable radicals were generated using a microsomal system whose hyperfine constants are the same as the radicals obtained by electrochemical reduction. The hyperfine patterns of quinones 2 and 3 were able to distinguish both regioisomers.

The theoretical results are in complete agreement with the experimental ones and helped to rationalize the small difference in the hyperfine constants.

Finally, the electron affinity calculated by the ADF level could be used to estimate the reduction potentials as a first approach to predict whether new drugs could have activity against *T. cruzi*.

Acknowledgements

This Research was supported by grants from EDID 99-02, TWAS 98039, FONDECYT 1000859 and FONDECYT 1000834.

References

[1] G.B. Henderson, P. Ulrich, A.H. Fairlamb, I. Rosenberg, M. Pereira, M. Sela, A Cerami, Proc. Natl. Acad. Sci. USA 85 (1988) 5374.
[2] B. Hazra, P. Sur, B. Sur, A. Banerjee, D.K. Roy, Planta Med. 51 (1984) 295.
[3] A. Morello, M. Pavani, J.A. Garbarino, M.C. Chamy, C. Frey, J. Mancilla, A. Guerrero, Y. Repetto, J. Ferreira, Comp. Biochem. Physiol. 112C (1995) 119.
[4] R. Docampo, S.N.J. Moreno, Rev. Infect. Dis. 6 (1984) 223.
[5] C. Olea-Azar, A. Atrua, R. di Maio, G. Seaone, H. Cerecetto, Spectrosc. Lett. 31 (1998) 849.
[6] A. Monge, A. Lopez de Cearin, E. Díaz, R. di Maio, M. Gonzalez, S. Onetto, G. Seaone, H. Cerecetto, C. Olea-Azar, J. Med. Chem. 42 (1999) 1941.
[7] C. Olea-Azar, A.A. Maria, M. Fernando, R. di Maio, G. Seoane, H. Cerecetto, Spectrosc. Lett. 31 (1998) 99.
[8] N.K. Cènas, D. Arscott, C.H. Jr. Williams, J.S. Blanchard, Biochemistry 33 (1994) 2509.
[9] M.O.F. Goulart, C.L. Zani, J. Tonholo, L.R. Freitas, F.C. de Abreu, A.B. De Oliveira, D.S. Raslan, S. Starling, E. Chiari, Bioorg. Med. Chem. Lett. 7 (1997) 2043.
[10] A. Korolkovas, Essentials of medicinal chemistry, 2nd, Wiley, New York, 1988.
[11] J.A. Valderrama, R. Araya-Maturana, F. Zuloaga, J. Chem. Soc. Perkin Trans. 1 (1993) 1103.
[12] R. Aranda, R. Araya-Maturana, M. Sauvain, V. Muñoz, E. Ruiz, E. Deharo, C. Moretti, Acta Andina 2 (1992) 125.
[13] Araya-Maturana R., Tropsha A. (unpublished results).
[14] R. Araya-Maturana, B.K. Cassels, T. Delgado-Castro, J.A. Valderrama, B.E. Weiss-Lopez, Tetrahedron 55 (1999) 637.
[15] M.J.S. Dewar, E.G. Zoebish, E.F. Healy, J.J.P. Steward, J. Am. Che. Soc. 107 (1985) 3902.
[16] S.H. Vosko, L. Wilk, J. Phys. Chem. B16 (1983) 3687.
[17] Perdew J. Phys. Recçv. B33, 8822.